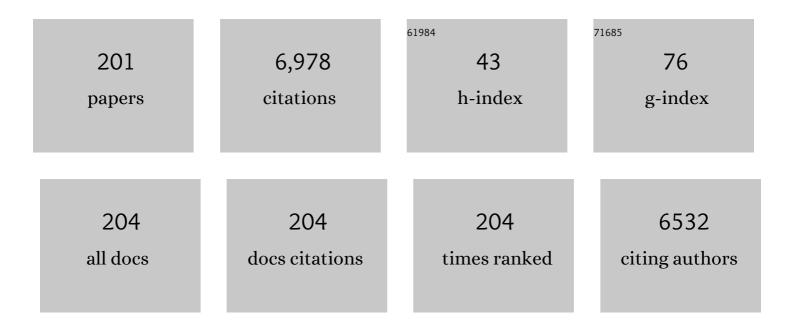
Andre Stesmans

List of Publications by Year in descending order

Source: https://exaly.com/author-pdf/1693492/publications.pdf Version: 2024-02-01



#	Article	IF	CITATIONS
1	Doping-induced ferromagnetism in InSe and SnO monolayers. Journal of Computational Electronics, 2021, 20, 88-94.	2.5	8
2	Measurement of direct and indirect bandgaps in synthetic ultrathin MoS2 and WS2 films from photoconductivity spectra. Journal of Applied Physics, 2021, 129, .	2.5	5
3	Internal photoemission of electrons from 2D semiconductor/3D metal barrier structures. Journal Physics D: Applied Physics, 2021, 54, 295101.	2.8	1
4	Dangling bond defects in silicon-passivated strained-Si1â^'xGex channel layers. Journal of Materials Science: Materials in Electronics, 2020, 31, 75-79.	2.2	0
5	Two-dimensional gallium and indium oxides from global structure searching: Ferromagnetism and half metallicity via hole doping. Journal of Applied Physics, 2020, 128, 034304.	2.5	12
6	Contact resistance at 2D metal/semiconductor heterostructures. Frontiers of Nanoscience, 2020, 17, 127-140.	0.6	0
7	Band alignment at interfaces of two-dimensional materials: internal photoemission analysis. Journal of Physics Condensed Matter, 2020, 32, 413002.	1.8	10
8	Variations of paramagnetic defects and dopants in geo-MoS2 from diverse localities probed by ESR. Journal of Chemical Physics, 2020, 152, 234702.	3.0	4
9	Analysis of Transferred MoS ₂ Layers Grown by MOCVD: Evidence of Mo Vacancy Related Defect Formation. ECS Journal of Solid State Science and Technology, 2020, 9, 093001.	1.8	9
10	First-Principles Study of the Contact Resistance at 2D Metal/2D Semiconductor Heterojunctions. Applied Sciences (Switzerland), 2020, 10, 2731.	2.5	7
11	Ferromagnetism and half-metallicity in two-dimensional <mml:math xmlns:mml="http://www.w3.org/1998/Math/MathML"><mml:mrow><mml:mi>M</mml:mi><mml:mi mathvariant="normal">O<mml:mo>Â</mml:mo><mml:mo>(</mml:mo><mml:mi>M</mml:mi><mml: monolayers induced by hole doping. Physical Review Materials, 2020, 4, .</mml: </mml:mi </mml:mrow></mml:math 	2.4 mo>= <td>ml:mo><mm< td=""></mm<></td>	ml:mo> <mm< td=""></mm<>
12	Contact Resistance at MoS ₂ -Based 2D Metal/Semiconductor Lateral Heterojunctions. ACS Applied Nano Materials, 2019, 2, 760-766.	5.0	19
13	Evaluation of the effective work-function of monolayer graphene on silicon dioxide by internal photoemission spectroscopy. Thin Solid Films, 2019, 674, 39-43.	1.8	7
14	Thermal stability and temperature dependent electron spin resonance characteristics of the As acceptor in geological 2H-MoS ₂ . Semiconductor Science and Technology, 2019, 34, 035022.	2.0	2
15	Energy Band Alignment of a Monolayer MoS 2 with SiO 2 and Al 2 O 3 Insulators from Internal Photoemission. Physica Status Solidi (A) Applications and Materials Science, 2019, 216, 1800616.	1.8	11
16	Aryl-viologen pentapeptide self-assembled conductive nanofibers. Chemical Communications, 2019, 55, 7354-7357.	4.1	12
17	Determination of energy thresholds of electron excitations at semiconductor/insulator interfaces using trap-related displacement currents. Microelectronic Engineering, 2019, 215, 110992.	2.4	3
18	Contact resistance at graphene/MoS2 lateral heterostructures. Applied Physics Letters, 2019, 114, .	3.3	14

#	Article	IF	CITATIONS
19	Impact of MoS ₂ layer transfer on electrostatics of MoS ₂ /SiO ₂ interface. Nanotechnology, 2019, 30, 055702.	2.6	11
20	On the chemistry and electrochemistry of LiPON breakdown. Journal of Materials Chemistry A, 2018, 6, 4848-4859.	10.3	44
21	Silicene on non-metallic substrates: Recent theoretical and experimental advances. Nano Research, 2018, 11, 1169-1182.	10.4	31
22	Internal Photoemission Metrology of Inhomogeneous Interface Barriers. Physica Status Solidi (A) Applications and Materials Science, 2018, 215, 1700865.	1.8	14
23	Band alignment at interfaces of synthetic few-monolayer MoS2 with SiO2 from internal photoemission. APL Materials, 2018, 6, .	5.1	17
24	Advances in SiCN-SiCN Bonding with High Accuracy Wafer-to-Wafer (W2W) Stacking Technology. , 2018, , .		24
25	Hole-Doped 2D InSe for Spintronic Applications. ACS Applied Nano Materials, 2018, 1, 6656-6665.	5.0	41
26	Two-Dimensional Crystal Grain Size Tuning in WS ₂ Atomic Layer Deposition: An Insight in the Nucleation Mechanism. Chemistry of Materials, 2018, 30, 7648-7663.	6.7	57
27	Ferromagnetism in two-dimensional hole-doped SnO. AIP Advances, 2018, 8, .	1.3	22
28	Nitrogen acceptor in 2H-polytype synthetic MoS2 assessed by multifrequency electron spin resonance. Journal of Vacuum Science and Technology A: Vacuum, Surfaces and Films, 2018, 36, .	2.1	5
29	Structural Properties of Al–O Monolayers in SiO ₂ on Silicon and the Maximization of Their Negative Fixed Charge Density. ACS Applied Materials & Interfaces, 2018, 10, 30495-30505.	8.0	30
30	Paramagnetic Intrinsic Defects in Polycrystalline Large-Area 2D MoS2 Films Grown on SiO2 by Mo Sulfurization. Nanoscale Research Letters, 2017, 12, 283.	5.7	12
31	(Invited) Internal Photoemission of Electrons from 2-Dimensional Semiconductors. ECS Transactions, 2017, 80, 191-201.	0.5	12
32	ESR identification of the nitrogen acceptor in 2H-polytype synthetic MoS2: Dopant level and activation. AIP Advances, 2017, 7, 105006.	1.3	10
33	Leakage current induced by surfactant residues in self-assembly based ultralow-k dielectric materials. Applied Physics Letters, 2017, 111, .	3.3	8
34	The lead acceptor in p-type natural 2H-polytype MoS ₂ crystals evidenced by electron paramagnetic resonance. Journal of Physics Condensed Matter, 2017, 29, 08LT01.	1.8	10
35	The Nitrogen Acceptor in 2Hâ€Polytype Synthetic MoS ₂ : Frequency and Temperature Dependent ESR Analysis. Physica Status Solidi C: Current Topics in Solid State Physics, 2017, 14, 1700211.	0.8	4
36	Controlled Sulfurization Process for the Synthesis of Large Area MoS ₂ Films and MoS ₂ /WS ₂ Heterostructures. Advanced Materials Interfaces, 2016, 3, 1500635.	3.7	61

#	Article	IF	CITATIONS
37	Electron energy distribution in Si/TiN and Si/Ru hybrid floating gates with hafnium oxide based insulators for charge trapping memory devices. Physica Status Solidi (A) Applications and Materials Science, 2016, 213, 265-269.	1.8	1
38	Photonic nanostructures for advanced light trapping in silicon solar cells: the impact of etching on the material electronic quality. Physica Status Solidi - Rapid Research Letters, 2016, 10, 158-163.	2.4	10
39	ESR study of p-type natural 2H-polytype MoS2 crystals: The As acceptor activity. Applied Physics Letters, 2016, 109, .	3.3	14
40	Band offsets and trap-related electron transitions at interfaces of (100)InAs with atomic-layer deposited Al2O3. Journal of Applied Physics, 2016, 120, 235701.	2.5	5
41	Silicene nanoribbons on transition metal dichalcogenide substrates: Effects on electronic structure and ballistic transport. Nano Research, 2016, 9, 3394-3406.	10.4	8
42	Effect of La doping on interface barrier between Si-passivated Ge and insulating HfO2. Physica Status Solidi C: Current Topics in Solid State Physics, 2016, 13, 855-859.	0.8	0
43	Oxygen and hydroxyl adsorption on MS ₂ (M = Mo, W, Hf) monolayers: a firstâ€principles molecular dynamics study. Physica Status Solidi - Rapid Research Letters, 2016, 10, 787-791.	2.4	7
44	Hydrogen induced dipole at the Pt/oxide interface in MOS devices. Physica Status Solidi (A) Applications and Materials Science, 2016, 213, 260-264.	1.8	5
45	Impact of point defects on the electronic and transport properties of silicene nanoribbons. Journal of Physics Condensed Matter, 2016, 28, 035302.	1.8	25
46	Topological to trivial insulating phase transition in stanene. Nano Research, 2016, 9, 774-778.	10.4	32
47	Electrical Characterization of Ultrathin RF-Sputtered LiPON Layers for Nanoscale Batteries. ACS Applied Materials & Interfaces, 2016, 8, 7060-7069.	8.0	63
48	Functional silicene and stanene nanoribbons compared to graphene: electronic structure and transport. 2D Materials, 2016, 3, 015001.	4.4	18
49	First-principles investigation of defects at GaAs/oxide interfaces. Materials Science in Semiconductor Processing, 2016, 42, 239-241.	4.0	1
50	Band alignment at interfaces of few-monolayer MoS2 with SiO2 and HfO2. Microelectronic Engineering, 2015, 147, 294-297.	2.4	31
51	High Cycling Stability and Extreme Rate Performance in Nanoscaled LiMn ₂ O ₄ Thin Films. ACS Applied Materials & Interfaces, 2015, 7, 22413-22420.	8.0	59
52	Band alignment and effective work function of atomic-layer deposited VO2 and V2 O5 films on SiO2 and Al2 O3. Physica Status Solidi C: Current Topics in Solid State Physics, 2015, 12, 238-241.	0.8	5
53	Inherent interface defects in thermal (211)Si/SiO2:29Si hyperfine interaction. , 2014, , .		0
54	Band alignment at interfaces of amorphous Al2O3 with Ge1â^'xSnx- and strained Ge-based channels. Applied Physics Letters, 2014, 104, 202107.	3.3	4

#	Article	IF	CITATIONS
55	Current-voltage characteristics of armchair Sn nanoribbons. Physica Status Solidi - Rapid Research Letters, 2014, 8, 931-934.	2.4	12
56	Magnetic defects in chemically converted graphene nanoribbons: electron spin resonance investigation. AIP Advances, 2014, 4, .	1.3	10
57	Reducing exciton-polaron annihilation in organic planar heterojunction solar cells. Physical Review B, 2014, 90, .	3.2	14
58	First-principles study of strained 2D MoS2. Physica E: Low-Dimensional Systems and Nanostructures, 2014, 56, 416-421.	2.7	119
59	Decreased Recombination Through the Use of a Nonâ€Fullerene Acceptor in a 6.4% Efficient Organic Planar Heterojunction Solar Cell. Advanced Energy Materials, 2014, 4, 1301413.	19.5	75
60	Large Area Carbon Nanosheet Capacitors. ECS Solid State Letters, 2014, 3, N8-N10.	1.4	5
61	Effect of Binder Content in Cu–In–Se Precursor Ink on the Physical and Electrical Properties of Printed CuInSe ₂ Solar Cells. Journal of Physical Chemistry C, 2014, 118, 27201-27209.	3.1	9
62	Modulation of electron barriers between Ti <scp>N</scp> _{<i>x</i>} and oxide insulators (<scp>S</scp> i <scp>O</scp> ₂ , Al ₂ <scp>O</scp> ₃) using Ti interlayer. Physica Status Solidi (A) Applications and Materials Science, 2014, 211, 382-388.	1.8	4
63	Influence of the bulkiness of the substituent on the aggregation and magnetic properties of poly(3â€alkylthiophene)s. Journal of Polymer Science Part A, 2014, 52, 76-86.	2.3	11
64	Multi-frequency electron spin resonance study of inherent Si dangling bond defects at the thermal (211)Si/SiO2interface. Physica Status Solidi C: Current Topics in Solid State Physics, 2014, 11, 1589-1592.	0.8	2
65	Generation of Si dangling bond defects at Si/insulator interfaces induced by oxygen scavenging. Physica Status Solidi (B): Basic Research, 2014, 251, 2193-2196.	1.5	4
66	Charge transition level of GeP _{b1} centers at interfaces of SiO ₂ /Ge _{<i>x</i>} Si _{1â[°]<i>x</i>} /SiO ₂ heterostructures investigated by positron annihilation spectroscopy. Physica Status Solidi (B): Basic Research, 2014, 251, 2211-2215.	1.5	1
67	The origin of white luminescence from silicon oxycarbide thin films. Applied Physics Letters, 2014, 104,	3.3	45
68	(Invited) Nature of Point Defects at High-Mobility Semiconductor/Interfaces Probed by Electron Spin Resonance: Thermal GaAs/GaAs-Oxide Structures. ECS Transactions, 2014, 64, 293-299.	0.5	0
69	Vibrational properties of epitaxial silicene layers on (111) Ag. Applied Surface Science, 2014, 291, 113-117.	6.1	49
70	Impact of strain on the passivation efficiency of Ge dangling bond interface defects in condensation grown SiO2/GexSi1â^'x/SiO2/(100)Si structures with nm-thin GexSi1â^'x layers. Applied Surface Science, 2014, 291, 11-15.	6.1	4
71	Processing-induced near-interfacial thermal donor generation in (100)Si/Si-oxycarbide insulator structures revealed by electron spin resonance. Physica Status Solidi C: Current Topics in Solid State Physics, 2014, 11, 1574-1577.	0.8	0
72	Vibrational properties of silicene and germanene. Nano Research, 2013, 6, 19-28.	10.4	144

#	Article	IF	CITATIONS
73	High-resolution electron spin resonance analysis of ion bombardment induced defects in advanced low-κ insulators (κ = 2.0-2.5). Applied Physics Letters, 2013, 102, .	3.3	15
74	Improved cathode buffer layer to decrease exciton recombination in organic planar heterojunction solar cells. Applied Physics Letters, 2013, 102, .	3.3	21
75	Chemical kinetics of the hydrogen-GePb1 defect interaction at the (100)GexSi1â^'x/SiO2 interface. Journal of Vacuum Science and Technology B:Nanotechnology and Microelectronics, 2013, 31, 010603.	1.2	3
76	Electron band alignment at the interface of (100)InSb with atomic-layer deposited Al ₂ O ₃ . Applied Physics Letters, 2012, 101, 082114.	3.3	11
77	Oxidation of the GaAs(001) surface: Insights from first-principles calculations. Physical Review B, 2012, 85, .	3.2	18
78	Near-interface Si substrate 3d metal contamination during atomic layer deposition processing detected by electron spin resonance. Journal of Applied Physics, 2012, 111, .	2.5	8
79	Interface nature of oxidized single-crystal arrays of etched Si nanowires on (100)Si. Applied Physics Letters, 2012, 100, 082110.	3.3	6
80	Correlation between interface traps and paramagnetic defects in c-Si/a-Si:H heterojunctions. Applied Physics Letters, 2012, 100, .	3.3	15
81	Interface barriers at the interfaces of polar GaAs(111) faces with Al2O3. Applied Physics Letters, 2012, 100, .	3.3	9
82	Semiconducting-like filament formation in TiN/HfO2/TiN resistive switching random access memories. Applied Physics Letters, 2012, 100, .	3.3	43
83	Electrically active defects at AlN/Si interface studied by DLTS and ESR. Physica Status Solidi (A) Applications and Materials Science, 2012, 209, 1851-1856.	1.8	17
84	Strain-induced semiconductor to metal transition in the two-dimensional honeycomb structure of MoS2. Nano Research, 2012, 5, 43-48.	10.4	620
85	Transitivity of band offsets between semiconductor heterojunctions and oxide insulators. Applied Physics Letters, 2011, 99, .	3.3	20
86	Inelastic electron tunneling spectroscopy of HfO2 gate stacks: A study based on first-principles modeling. Applied Physics Letters, 2011, 99, 132101.	3.3	0
87	Electronic properties of hydrogenated silicene and germanene. Applied Physics Letters, 2011, 98, .	3.3	399
88	Universal stress-defect correlation at (100)semiconductor/oxide interfaces. Applied Physics Letters, 2011, 98, 141901.	3.3	10
89	TiN x / HfO 2 interface dipole induced by oxygen scavenging. Applied Physics Letters, 2011, 98, .	3.3	34
90	Band Alignment at Interfaces of Oxide Insulators with Semiconductors. Integrated Ferroelectrics, 2011, 125, 53-60.	0.7	5

6

#	Article	IF	CITATIONS
91	Interface state energy distribution and Pb defects at Si(110)/SiO2 interfaces: Comparison to (111) and (100) silicon orientations. Journal of Applied Physics, 2011, 109, .	2.5	61
92	First-principles study of Ge dangling bonds in GeO2 and correlation with electron spin resonance at Ge/GeO2 interfaces. Applied Physics Letters, 2011, 99, .	3.3	11
93	Influence of Al ₂ O ₃ crystallization on band offsets at interfaces with Si and TiN _x . Applied Physics Letters, 2011, 99, 072103.	3.3	50
94	Electron band alignment at the interface of (100)GaSb with molecular-beam deposited Al2O3. Applied Physics Letters, 2011, 98, 072102.	3.3	7
95	Structural and vibrational properties of amorphous GeO2 from first-principles. Applied Physics Letters, 2011, 98, .	3.3	6
96	Electronic structure of NiO layers grown on Al2O3 and SiO2 using metallo-organic chemical vapour deposition. Journal of Applied Physics, 2011, 110, .	2.5	4
97	Defects in Low-k Insulators (κ=2.5 – 2.0): ESR Analysis and Charge Injection. Materials Research Society Symposia Proceedings, 2011, 1335, 119.	0.1	3
98	Electron energy band alignment at the NiO/SiO2 interface. Applied Physics Letters, 2010, 96, .	3.3	7
99	Comparative electron spin resonance study of epi-Lu2O3/(111)Si and a-Lu2O3/(100)Si interfaces: Misfit point defects. Journal of Applied Physics, 2010, 107, 094502.	2.5	4
100	Electron energy band alignment at the (100)Si/MgO interface. Applied Physics Letters, 2010, 96, .	3.3	11
101	Pb(0) centers at the Si-nanocrystal/SiO2 interface as the dominant photoluminescence quenching defect. Journal of Applied Physics, 2010, 107, 084309.	2.5	41
102	Influence of <i>in situ</i> applied ultrasound during Si+ implantation in SiO2 on paramagnetic defect generation. Journal of Applied Physics, 2010, 107, .	2.5	11
103	Low temperature silicon dioxide by thermal atomic layer deposition: Investigation of material properties. Journal of Applied Physics, 2010, 107, .	2.5	86
104	Can silicon behave like graphene? A first-principles study. Applied Physics Letters, 2010, 97, .	3.3	208
105	Magnetic Properties of Substituted Poly(thiophene)s in Their Neutral State. Macromolecules, 2010, 43, 2910-2915.	4.8	13
106	Electron band alignment between (100)InP and atomic-layer deposited Al2O3. Applied Physics Letters, 2010, 97, 132112.	3.3	17
107	Nitrogen at the <mml:math <br="" xmlns:mml="http://www.w3.org/1998/Math/MathML">display="inline"><mml:mrow><mml:mtext>Si-nanocrystal</mml:mtext><mml:mo>/</mml:mo><ml:msub><m and its influence on luminescence and interface defects. Physical Review B, 2010, 82, .</m </ml:msub></mml:mrow></mml:math>	ml:m20w>	<mml:mtext></m
108	Electronic properties of two-dimensional hexagonal germanium. Applied Physics Letters, 2010, 96, .	3.3	114

108 Electronic properties of two-dimensional hexagonal germanium. Applied Physics Letters, 2010, 96, .

#	Article	IF	CITATIONS
109	A theoretical study of the initial oxidation of the GaAs(001)-β2(2×4) surface. Applied Physics Letters, 2009, 95, .	3.3	31
110	Nontrigonal Ge dangling bond interface defect in condensation-grown <mml:math xmlns:mml="http://www.w3.org/1998/Math/MathML" display="inline"><mml:mrow><mml:mrow><mml:mo>(</mml:mo><mml:mrow><mml:mn>100</mml:mn>Physical Review B, 2009, 79, .</mml:mrow></mml:mrow></mml:mrow></mml:math 	mrów> <m< td=""><td>າກີ່!?mo>)</td></m<>	າ ກີ່!? mo>)
111	Valence band energy in confined Si1â^'xGex (0.28 <x<0.93) 172106.<="" 2009,="" 94,="" applied="" layers.="" letters,="" physics="" td=""><td>3.3</td><td>18</td></x<0.93)>	3.3	18
112	Electronic properties of Ge dangling bond centers at Si1â^'xGex/SiO2 interfaces. Applied Physics Letters, 2009, 95, 222106.	3.3	17
113	First-principles study of the electronic properties of Ge dangling bonds at (100)Si1â^'xGex/SiO2 interfaces. Applied Physics Letters, 2009, 95, .	3.3	10
114	Energy barriers at interfaces between (100) InxGa1â^'xAsâ€^(â‰ ¤ â‰ 9 .53) and atomic-layer deposited Al2O3 and HfO2. Applied Physics Letters, 2009, 94, .	3.3	24
115	Electron spin resonance observation of an interfacial Ge <i>P</i> _{<i>b</i>1} -type defect in SiO ₂ <i>/</i> (100)Si _{1â^'<i>x</i>} Ge _{<i>x</i>} <i>/Colored and the set of th</i>	'i 1.5 8	10
116	Alternative techniques to reduce interface traps in nâ€ŧype 4H‣iC MOS capacitors. Physica Status Solidi (B): Basic Research, 2008, 245, 1378-1389.	1.5	64
117	Electronic structure of the interface of aluminum nitride with Si(100). Journal of Applied Physics, 2008, 104, 093713.	2.5	25
118	Paramagnetic point defects at interfacial layers in biaxial tensile strained (100)Si/SiO2. Journal of Applied Physics, 2008, 103, .	2.5	17
119	Paramagnetic point defects at SiO2/nanocrystalline Si interfaces. Applied Physics Letters, 2008, 93, .	3.3	22
120	Photoconductivity of Hf-based binary metal oxide systems. Journal of Applied Physics, 2008, 104, 114103.	2.5	12
121	Misfit point defects at the epitaxial Lu2O3/(111)Si interface revealed by electron spin resonance. Applied Physics Letters, 2008, 93, 103505.	3.3	4
122	Beneficial effect of La on band offsets in Ge/high- \hat{I}^{e} insulator structures with GeO2 and La2O3 interlayers. Applied Physics Letters, 2008, 93, 102115.	3.3	16
123	The effect of implanting boron on the optical absorption and electron paramagnetic resonance spectra of silica. Journal of Applied Physics, 2008, 104, 054110.	2.5	2
124	Influence of metal capping layer on the work function of Mo gated metal-oxide semiconductor stacks. Applied Physics Letters, 2008, 93, 083511.	3.3	3
125	Energy barriers at interfaces of (100)GaAs with atomic layer deposited Al2O3 and HfO2. Applied Physics Letters, 2008, 93, .	3.3	30
126	Internal photoemission of electrons from Ta-based conductors into SiO2 and HfO2 insulators. Journal of Applied Physics, 2008, 104, .	2.5	7

#	Article	IF	CITATIONS
127	Internal photoemission at interfaces of high- $\hat{I}^{\rm e}$ insulators with semiconductors and metals. Journal of Applied Physics, 2007, 102, .	2.5	223
128	Analysis of the (100)Si/LaAlO3 structure by electron spin resonance: nature of the interface. Journal of Materials Science: Materials in Electronics, 2007, 18, 735-741.	2.2	0
129	Ruthenium gate electrodes on SiO2 and HfO2: Sensitivity to hydrogen and oxygen ambients. Applied Physics Letters, 2006, 88, 243514.	3.3	44
130	Probing Semiconductor/Insulator Heterostructures Through Electron Spin Resonance of Point Defects: Interfaces, Interlayers, and Stress. Materials Research Society Symposia Proceedings, 2006, 984, 1.	0.1	0
131	High open-circuit voltage values on fine-grained thin-film polysilicon solar cells. Journal of Applied Physics, 2006, 100, 063702.	2.5	41
132	Effective work function modulation by controlled dielectric monolayer deposition. Applied Physics Letters, 2006, 89, 113505.	3.3	29
133	Reaction-dispersive proton transport model for negative bias temperature instabilities. Applied Physics Letters, 2005, 86, 093506.	3.3	51
134	Interface traps and dangling-bond defects in (100)Geâ^•HfO2. Applied Physics Letters, 2005, 87, 032107.	3.3	119
135	Defect generation in high κ gate dielectric stacks under electrical stress: the impact of hydrogen. Journal of Physics Condensed Matter, 2005, 17, S2075-S2088.	1.8	33
136	Conduction band-edge States associated with the removal of d-state degeneracies by the Jahn-Teller effect. IEEE Transactions on Device and Materials Reliability, 2005, 5, 65-83.	2.0	63
137	Energy band alignment at the (100)Ge/HfO2 interface. Applied Physics Letters, 2004, 84, 2319-2321.	3.3	107
138	Stable trapping of electrons and holes in deposited insulating oxides: Al2O3, ZrO2, and HfO2. Journal of Applied Physics, 2004, 95, 2518-2526.	2.5	74
139	Vacancy clusters in diamond studied by electron spin resonance. Physica Status Solidi A, 2004, 201, 2509-2515.	1.7	10
140	Energy distribution of the (100)Si/HfO2 interface states. Applied Physics Letters, 2004, 84, 4771-4773.	3.3	30
141	Si dangling-bond-type defects at the interface of (100)Si with ultrathin HfO2. Applied Physics Letters, 2003, 82, 4074-4076.	3.3	91
142	Invasive nature of corona charging on thermal Si/SiO2 structures with nanometer-thick oxides revealed by electron spin resonance. Applied Physics Letters, 2003, 82, 2835-2837.	3.3	23
143	Pb-type interface defects in (100)Si/SiO2 structures grown in ozonated water solution. Journal of Applied Physics, 2003, 93, 4331-4333.	2.5	2
144	Annealing Induced Degradation of Thermal SiO2On (100)Si: Point Defect Generation. Radiation Effects and Defects in Solids, 2003, 158, 419-425.	1.2	1

9

#	Article	IF	CITATIONS
145	Si dangling-bond-type defects at the interface of (100)Si with ultrathin layers of SiOx, Al2O3, and ZrO2. Applied Physics Letters, 2002, 80, 1957-1959.	3.3	92
146	Influence of interface relaxation on passivation kinetics in H2 of coordination Pb defects at the (111)Si/SiO2 interface revealed by electron spin resonance. Journal of Applied Physics, 2002, 92, 1317-1328.	2.5	63
147	Characterization of S centers generated by thermal degradation in SiO2 on (100)Si. Applied Physics Letters, 2002, 80, 4753-4755.	3.3	4
148	Hole trapping in ultrathin Al2O3 and ZrO2 insulators on silicon. Applied Physics Letters, 2002, 80, 1261-1263.	3.3	35
149	Defects at the interface of (100)Si with ultrathin layers of SiO[sub x], Al[sub 2]O[sub 3], and ZrO[sub 2] probed by electron spin resonance. Journal of Vacuum Science & Technology an Official Journal of the American Vacuum Society B, Microelectronics Processing and Phenomena, 2002, 20, 1720.	1.6	11
150	ESR and Photo-ESR Study of Defects in CVD Diamond. Physica Status Solidi A, 2002, 193, 448-456.	1.7	13
151	Synthesis and characterization of sol-gel derived ZnS : Mn2+ nanocrystallites embedded in a silica matrix. Bulletin of Materials Science, 2002, 25, 175-180.	1.7	105
152	Band alignments in metal–oxide–silicon structures with atomic-layer deposited Al2O3 and ZrO2. Journal of Applied Physics, 2002, 91, 3079-3084.	2.5	190
153	Microcharacterization of Defects Induced in Fused Silica by High Power 3ï‰ UV (355nm) Laser Pulses. Microscopy and Microanalysis, 2001, 7, 496-497.	0.4	0
154	Comment on "Do Pb1 centers have levels in the Si band gap? Spin-dependent recombination study of the Pb1 â€~hyperfine spectrum' ―[Appl. Phys. Lett. 76, 3771 (2000)]. Applied Physics Letters, 2001, 78, 145	1- 1 452.	7
155	Model for the charge trapping in high permittivity gate dielectric stacks. Journal of Applied Physics, 2001, 89, 792-794.	2.5	32
156	Interaction of Pb defects at the (111)Si/SiO2 interface with molecular hydrogen: Simultaneous action of passivation and dissociation. Journal of Applied Physics, 2000, 88, 489-497.	2.5	99
157	Pressure dependence of Si/SiO2 degradation suppression by helium. Journal of Applied Physics, 2000, 87, 7338-7341.	2.5	8
158	Paramagnetic defects at the interface of ultrathin oxides grown under vacuum ultraviolet photon excitation on (111) and (100) Si. Applied Physics Letters, 2000, 77, 1469-1471.	3.3	35
159	Dissociation kinetics of hydrogen-passivatedPbdefects at the(111)Si/SiO2interface. Physical Review B, 2000, 61, 8393-8403.	3.2	120
160	Valence band offset and hole injection at the 4H-, 6H-SiC/SiO2 interfaces. Applied Physics Letters, 2000, 77, 2024-2026.	3.3	35
161	Hydrogenâ€Related Leakage Currents Induced in Ultrathin SiO2 / Si Structures by Vacuum Ultraviolet Radiation. Journal of the Electrochemical Society, 1999, 146, 3409-3414.	2.9	37
162	Blockage of the annealing-induced Si/SiO2 degradation by helium. Applied Physics Letters, 1999, 74, 1009-1011.	3.3	7

#	Article	IF	CITATIONS
163	Correlation Between Development of Leakage Current and Hydrogen Ionization in Ultrathin Silicon Dioxide Layers. Materials Research Society Symposia Proceedings, 1999, 592, 203.	0.1	1
164	Thermally induced interface degradation in (100) and (111) Si/SiO[sub 2] analyzed by electron spin resonance. Journal of Vacuum Science & Technology an Official Journal of the American Vacuum Society B, Microelectronics Processing and Phenomena, 1998, 16, 3108.	1.6	47
165	Electron spin resonance features of interface defects in thermal (100)Si/SiO2. Journal of Applied Physics, 1998, 83, 2449-2457.	2.5	164
166	Electrical activity of interfacial paramagnetic defects in thermal (100)Si/SiO2. Physical Review B, 1998, 57, 10030-10034.	3.2	111
167	Positive charging of thermal SiO2/(100)Si interface by hydrogen annealing. Applied Physics Letters, 1998, 72, 79-81.	3.3	40
168	Hydrogen-induced thermal interface degradation in (111) Si/SiO2 revealed by electron-spin resonance. Applied Physics Letters, 1998, 72, 2271-2273.	3.3	44
169	Electrical conduction of buried SiO2 layers analyzed by photon stimulated electron tunneling. Applied Physics Letters, 1997, 70, 1260-1262.	3.3	10
170	Interfacial Defects in SiO2Revealed by Photon Stimulated Tunneling of Electrons. Physical Review Letters, 1997, 78, 2437-2440.	7.8	107
171	H-complexed oxygen vacancy in SiO2: Energy level of a negatively charged state. Applied Physics Letters, 1997, 71, 3844-3846.	3.3	42
172	Trap Generation in Buried Oxides of Siliconâ€onâ€Insulator Structures by Vacuum Ultraviolet Radiation. Journal of the Electrochemical Society, 1997, 144, 749-753.	2.9	5
173	Electron states and microstructure of thina-C:H layers. Physical Review B, 1996, 54, 10820-10826.	3.2	49
174	Elimination of SiC/SiO2 interface states by preoxidation ultravioletâ€ozone cleaning. Applied Physics Letters, 1996, 68, 2141-2143.	3.3	116
175	Annealing induced degradation of thermal SiO2: S center generation. Applied Physics Letters, 1996, 69, 2056-2058.	3.3	39
176	Hole traps in oxide layers thermally grown on SiC. Applied Physics Letters, 1996, 69, 2252-2254.	3.3	47
177	Thermally induced interface degradation in (111) Si/SiO2traced by electron spin resonance. Physical Review B, 1996, 54, R11129-R11132.	3.2	72
178	Electron-spin-resonance analysis of the natural intrinsicEXcenter in thermalSiO2on Si. Physical Review B, 1995, 51, 4987-4997.	3.2	18
179	Impact of supplemental implantation of oxygen on defect centers in the separation by implantation of oxygen structure. Applied Physics Letters, 1995, 67, 1399-1401.	3.3	3
180	Degradation of the thermal oxide of the Si/SiO2/Al system due to vacuum ultraviolet irradiation. Journal of Applied Physics, 1995, 78, 6481-6490.	2.5	65

1

#	Article	IF	CITATIONS
181	Positive charging of buried SiO2by hydrogenation. Applied Physics Letters, 1994, 64, 2575-2577.	3.3	32
182	Generation aspects of the delocalized intrinsicEXdefect in thermal SiO2. Journal of Applied Physics, 1994, 75, 1047-1058.	2.5	38
183	Structural relaxation ofPbdefects at the (111)Si/SiO2interface as a function of oxidation temperature: ThePb-generation–stress relationship. Physical Review B, 1993, 48, 2418-2435.	3.2	192
184	Characterization and depth profiling ofE' defects in buried SiO2. Journal of Applied Physics, 1993, 74, 275-283.	2.5	81
185	Shallow donor in separation by implantation of oxygen structures revealed by electricâ€field modulated electron spin resonance. Applied Physics Letters, 1993, 62, 273-275.	3.3	12
186	Defect generation sensitivity depth profile in buried SiO2using Ar plasma exposure. Applied Physics Letters, 1993, 62, 2277-2279.	3.3	9
187	Electron spin resonance characterization and localization of a thermally generated donor inherent to the separation by implantation of oxygen process. Journal of Applied Physics, 1993, 73, 876-889.	2.5	11
188	Observation of a delocalizedE' center in buried SiO2. Applied Physics Letters, 1993, 62, 2405-2407.	3.3	26
189	Depth Profiling of Oxygen Vacancy Defect Generation in Buried SiO ₂ . Materials Research Society Symposia Proceedings, 1992, 284, 299.	0.1	4
190	Localization and Electric-Field Modulated Electron Spin Resonance of a Shallow Donor in Simox. Materials Research Society Symposia Proceedings, 1992, 284, 573.	0.1	0
191	Chemical etch rates in HF solutions as a function of thickness of thermal SiO2and buried SiO2formed by oxygen implantation. Journal of Applied Physics, 1991, 69, 6656-6664.	2.5	30
192	Dissimilarity between thermal oxide and buried oxide fabricated by implantation of oxygen on Si revealed by etch rates in HF. Applied Physics Letters, 1990, 57, 2250-2252.	3.3	9
193	Maximum density ofPbcenters at the (111) Si/SiO2interface after vacuum anneal. Applied Physics Letters, 1990, 57, 2663-2665.	3.3	37
194	The application of submetallic phosphorus-doped Si as ESR marker. Journal of Magnetic Resonance, 1988, 76, 14-21.	0.5	14
195	Evidence for a phase-transition-induced change in the surface spin-flip probability of conduction electrons from CESR on n-irradiated, LIF; its application as an intensity reference. Journal Physics D: Applied Physics, 1988, 21, 1205-1214.	2.8	18
196	Magnetism of neutron-damaged alpha-quartz. Radiation Effects, 1986, 97, 183-190.	0.4	3
197	Buried oxide inhomogeneity in low-dose SIMOX structures. , 0, , .		0

198 Influence of gamma irradiation on ESR active defects in SIMOX structures. , 0, , .

#	Article	IF	CITATIONS
199	Hydrogen Induced Positive Charging of Buried SiO/sub 2/. , 0, , .		1
200	[100]Si with ultrathin layers of SiO/sub 2/, Al/sub 2/O/sub 3/, and ZrO/sub 2/: electron spin resonance study. , 0, , .		0
201	Electrical and physical characterization of high-k dielectric layers. , 0, , .		3